Use of Sea Level Observations to Estimate Salinity Variability in the Tropical Pacific

FEMKE C. VOSSEPOEL*

Delft Institute for Earth-Oriented Space Research, Delft University of Technology, Netherlands, and NOAA/Laboratory for Satellite Altimetry, Silver Spring, Maryland

RICHARD W. REYNOLDS

National Centers for Environmental Prediction, Camp Springs, Maryland

LAURY MILLER

NOAA/Laboratory for Satellite Altimetry, Silver Spring, Maryland

ABSTRACT

The equatorial sea level analysis of the National Centers for Environmental Predictions deviates by as much as 8 cm from independent TOPEX/Poseidon (T/P) observations. This may be due to the model's underestimation of salinity variability. Therefore, methods are developed to improve the model's salinity field through T/P data assimilation and use of sea surface salinity (SSS) observations.

In regions where temperature is well known, salinity estimates are made with the use of climatological temperature–salinity (T–S) correlations. These estimates are improved by combining T–S with SSS observations and corrected with dynamic height, which provides information on salinity variability. Tests with independent conductivity temperature depth data show that the combination of T–S with SSS significantly improves salinity estimates. In the western Pacific, the maximum root-mean-square (rms) estimation error of 0.55 psu is reduced to 0.42 psu by the use of SSS in the salinity estimate. Correction with dynamic height reduces this rms to 0.22 psu. Also in other parts of the tropical Pacific Ocean the salinity estimation errors are reduced by a factor of 2 by combination of the T–S estimate with SSS and dynamic height. This study provides the first step toward an assimilation scheme in which salinity is corrected with the use of T/P sea level observations.

1. Introduction

While dynamic height can be computed from temperature and salinity profiles, it can also be estimated from altimetric sea level observations. Of course, dynamic height and sea level are not equivalent: dynamic height captures all baroclinic processes above a reference level of specific pressure, while sea level also includes the motions below this reference level and barotropic processes. Despite these differences, sea level observations from TOPEX/Poseidon (T/P) form a good proxy for dynamic height in the tropical Pacific (Katz et al. 1995).

To improve the model's analysis of dynamic height, T/P observations are used for data assimilation in the operational ocean general circulation model (OGCM) at the National Centers for Environmental Prediction (NCEP) (Ji et al. 1995). In the assimilation, changes in dynamic height are attributed to changes in temperature. Although this assumption is commonly made, it may introduce errors in regions where salinity fluctuations contribute significantly to dynamic height variability. This is particularly the case for the western tropical Pacific, where dynamic height errors due to misestimation of salinity reach values of 6 dyn cm (e.g., Donguy et al. 1986; Delcroix et al. 1987).

For consistent model dynamics, both temperature and salinity variations should be monitored. A recent modeling study by Murtugudde and Busalacchi (1998) points out that the role of salinity should not be neglected in tropical ocean dynamics. The importance of including salinity in data assimilation has been addressed by Cooper (1988) and Woodgate (1997). Cooper (1988) demonstrates in a tropical ocean model that univariate assimilation of either temperature or salinity data alone would seriously bias the density field, resulting

* Additional affiliation: Royal Netherlands Meteorological Institute, De Bilt, Netherlands.

Corresponding author address: Dr. Femke C. Vossepoel, Delft University of Technology, Faculty of Aerospace Engineering, Room 911, Kluyverweg, 1 2629 HS, Delft, Netherlands.
E-mail: f.vossepoel@lr.tudelft.nl

in a model velocity field less accurate than when no data at all were assimilated. He thereby illustrates that the lack of salinity data in a model in which temperature is being assimilated results in temperature data being of little use. Assimilation of temperature data improves the temperature analysis, but at the same time, it may worsen the analysis of other fields, such as velocity.

The experiments of Cooper (1988) are interesting in the light of the success of T/P data assimilation for ocean initialization, as discussed by Ji et al. (1999). With respect to the forecast of the 1997 El Niño, Ji et al. (1998) compare different runs: one run in which temperature data are assimilated (NCEP–XBT), and one run in which both temperature and T/P data are assimilated (NCEP–T/P). The NCEP–T/P run gives remarkably better forecasts than the NCEP–XBT run. This result suggests that the inclusion of sea level data improves the initial conditions for the forecast run because the density is improved. But is the density really optimized? In both assimilation runs, the density is adjusted by correction of temperature. However, according to the results of Cooper (1988), the density field would be truly optimized if not only temperature but also salinity were corrected. Because salinity data are not as widely available as temperature data, there are fewer salinity observations to assimilate. An alternative approach needs to be found to improve the salinity variability in the ocean model.

In places where temperature is well known, T/P sea level could be used to correct the salinity estimate. This application of altimetry would improve the model dynamic height as well as the model temperature and salinity field. This would result in a more realistic representation of the density and possibly of the velocity fields. A key problem in the salinity data assimilation is how to estimate salinity as a function of depth without any direct salinity observations. A widely accepted approach for salinity estimation is the use of climatological temperature–salinity (T–S) correlations, provided by historical temperature and salinity datasets (Emery and Dewar 1982; Levitus and Boyer 1994; Levitus et al. 1994). These correlations are commonly used to track water masses, assuming that for every water mass the T–S correlation is applicable. In theory, knowing one of the density components T or S, one could infer the other component using climatological T–S correlations. In practice, T–S correlations are not constant but vary with time (see, e.g., Donguy 1994). Consequently, the use of T–S for the estimation of salinity will not be completely accurate.

Techniques have been developed to improve the T–S estimate with the use of sea surface salinity (SSS) observations (Donguy et al. 1986; Kessler and Taft 1987). However, even with the use of SSS, the salinity estimate contains errors. If temperature is well known, and barotropic variations in dynamic height are negligible, then differences between sea level from T/P and dynamic height estimated from temperature and salinity generated by T–S can be largely attributed to errors in the salinity estimation. In this paper we will identify the errors made in the salinity estimate and investigate the feasibility of the use of sea surface salinity and sea level observations to improve this estimate. To ensure sufficient temperature observations, the domain of our study will be limited to the tropical Pacific, between 10°N and 10°S, where moored buoys provide good temperature coverage.

This work is organized as follows. Section 2 gives an overview of the variability of salinity in the tropical Pacific and its relationship to temperature variability. Next, the procedure for salinity estimation and correction is presented in section 3. The salinity estimation with T–S relationships and SSS observations is described in section 4, followed by the salinity correction with dynamic height in section 5. The salinity estimation and correction methods are tested with independent conductivity–temperature–depth (CTD) data in section 6. Section 7 summarizes the salinity estimation and correction methods and discusses different aspects of the use of altimeter data for salinity estimation. Eventually, the above-mentioned techniques will be used to improve model salinities, as part of a comprehensive assimilation scheme. Details on the assimilation scheme and its implementation, however, are beyond the scope of this work.

2. Salinity variability in the tropical Pacific

Although T–S relationships are commonly used in the computation of dynamic height, the assumption that salinity can be described as a function of temperature is not always valid. In this section we use the historical hydrographic dataset compiled by Ando and McPhaden (1997) to identify those regions in the equatorial Pacific where the estimation of salinity by means of T–S will be most or least accurate. The dataset includes approximately 9000 CTD profiles from research cruises in the equatorial Pacific during 1975–96 and is maintained by the National Oceanic and Atmospheric Administration/Pacific Marine Environmental Laboratory (NOAA/PMEL). The spatial distribution of the CTDs is illustrated in Fig. 1. For details on the space and time sampling, see Ando and McPhaden (1997).

To quantify the salinity and temperature variability, the salinity and temperature mean and standard deviation were determined from the hydrographic data for three different regions: the western Pacific (120°E–180°, Fig. 2), the central Pacific, (120°W–180°, Fig. 3), and the eastern Pacific (80°–120°W, Fig 4.).

The mean salinity field of the tropical Pacific exhibits a subsurface salinity maximum in the Southern Hemisphere, which is clearly visible in the mean salinity field for the western Pacific (Fig. 2). This high salinity water in the middle of the thermocline is sometimes denoted as Tropical Water following Tsuchiya et al. (1989). The Tropical Water originates at the surface around the Trop-

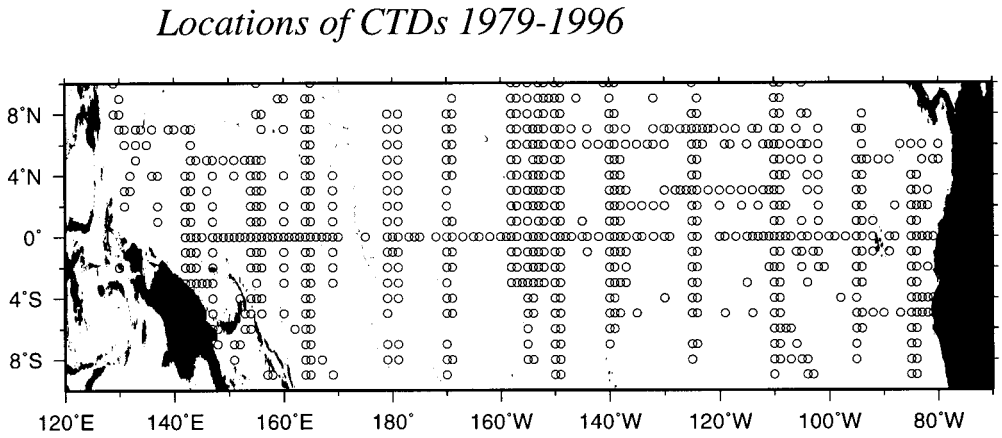

FIG. 1. The location of all CTDs in the Ando and McPhaden (1997) dataset in the equatorial Pacific. The profiles are grouped in 1° bins.

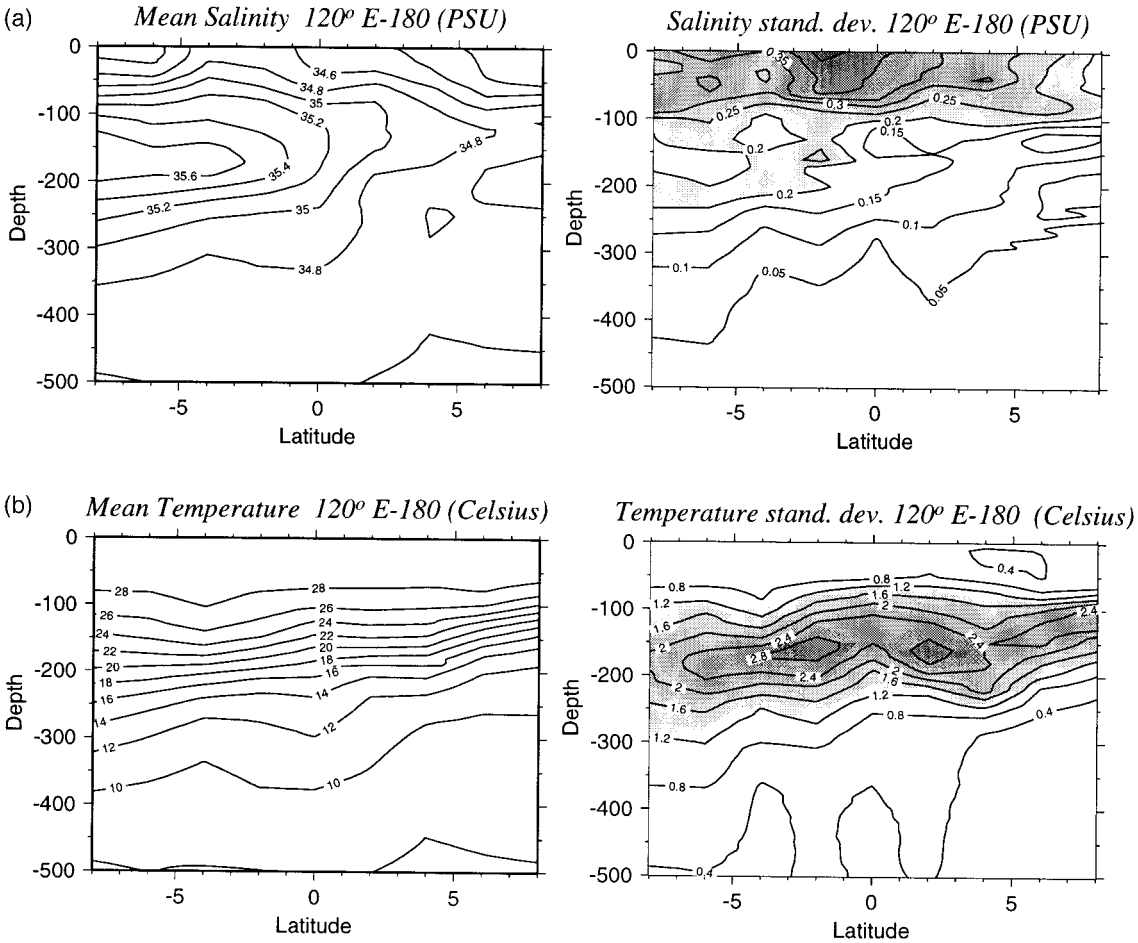

FIG. 2. Mean and standard deviation of the salinity and temperature in the western Pacific (120°E–180°) based on hydrographic data (1979–96) as a function of depth and latitude. (a) In the salinity standard deviation plot values exceeding 0.2 psu are shaded, contours are drawn at 0.05 psu intervals. (b) For the temperature plot, standard deviation values of 1.2°C and above are shaded. Contours are drawn every 0.2°C.

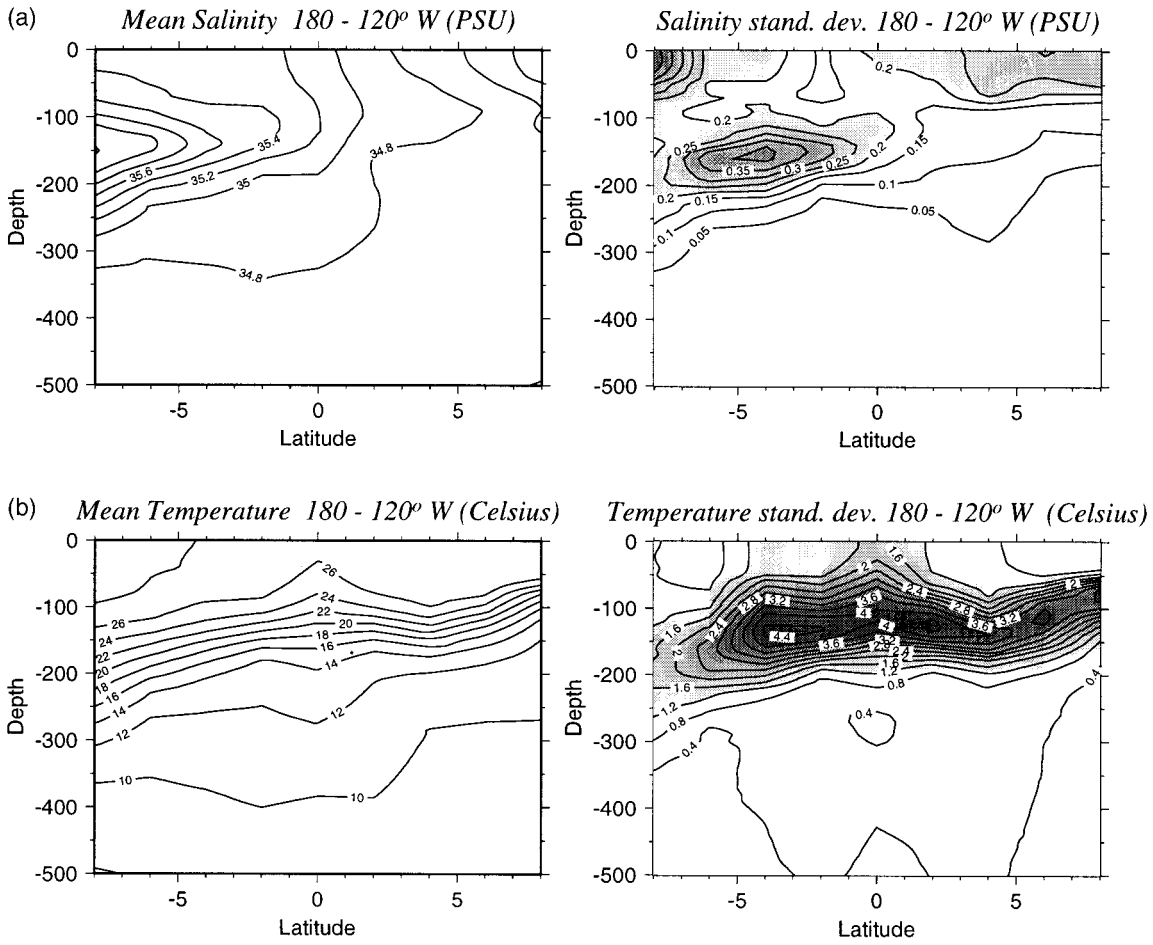

FIG. 3. (a) Mean and standard deviation salinity and (b) temperature. As in Fig. 2, but for the central Pacific (120°W–180°).

ic of Capricorn in the South Pacific, where salty surface waters are subducted while traveling westward and equatorward (see, e.g., Tsuchiya 1968; Tsuchiya et al. 1989; Donguy 1994).

The standard deviation of salinity reaches a maximum of 0.45 psu at the surface (Fig. 2). On the other hand, the standard deviation of temperature at the surface is relatively low. The maximum of the standard deviation of temperature is located at the mean depth of the thermocline and is related to vertical displacements of the thermocline. Salinity variability in this region is independent of temperature variability and is probably due to advection and precipitation (e.g., Xie and Arkin 1997).

Independent behavior of salinity and temperature in the upper layer of the western Pacific is described by Godfrey and Lindstrom (1989). Differences in stratification of temperature and salinity are associated with the formation of a salinity gradient barrier in the isothermal layer. Lukas and Lindstrom (1991) showed that this ''barrier layer'' prohibits surface fluxes to influence the ocean below the halocline and significantly affects the available heat in the upper ocean. Such a barrier layer is not an incidental phenomenon, but a climatological feature of all tropical oceans, especially where rainfall is heavy (Sprintall and Tomczak 1992). The formation and the physical importance of the barrier layer have been discussed based on observations (e.g., Godfrey and Lindstrom 1989; McPhaden and Hayes 1990; Ando and McPhaden 1997). Even though recent progress has been made in the modeling of the barrier layer (You 1998; Shinoda and Lukas 1995; Vialard and Delecluse 1998a, b; Anderson et al. 1996), its relationship to other mixed layer processes has yet to be quantified.

Clearly, the salinity stratification in the isothermal layer complicates the use of a climatological T–S for salinity estimation in the mixed layer (e.g., Morris et al. 1998). The use of T–S is also complicated at depths below the mixed layer in the western Pacific because T–S correlations vary with time. Donguy (1994) described the variability of T–S in the western tropical Pacific in relation to El Niño–Southern Oscillation (ENSO) variability. With the use of hydrographic datasets, he illustrated that the subsurface salinity maximum in the western Pacific is zonally advected and becomes stronger and shallower after an El Niño event.

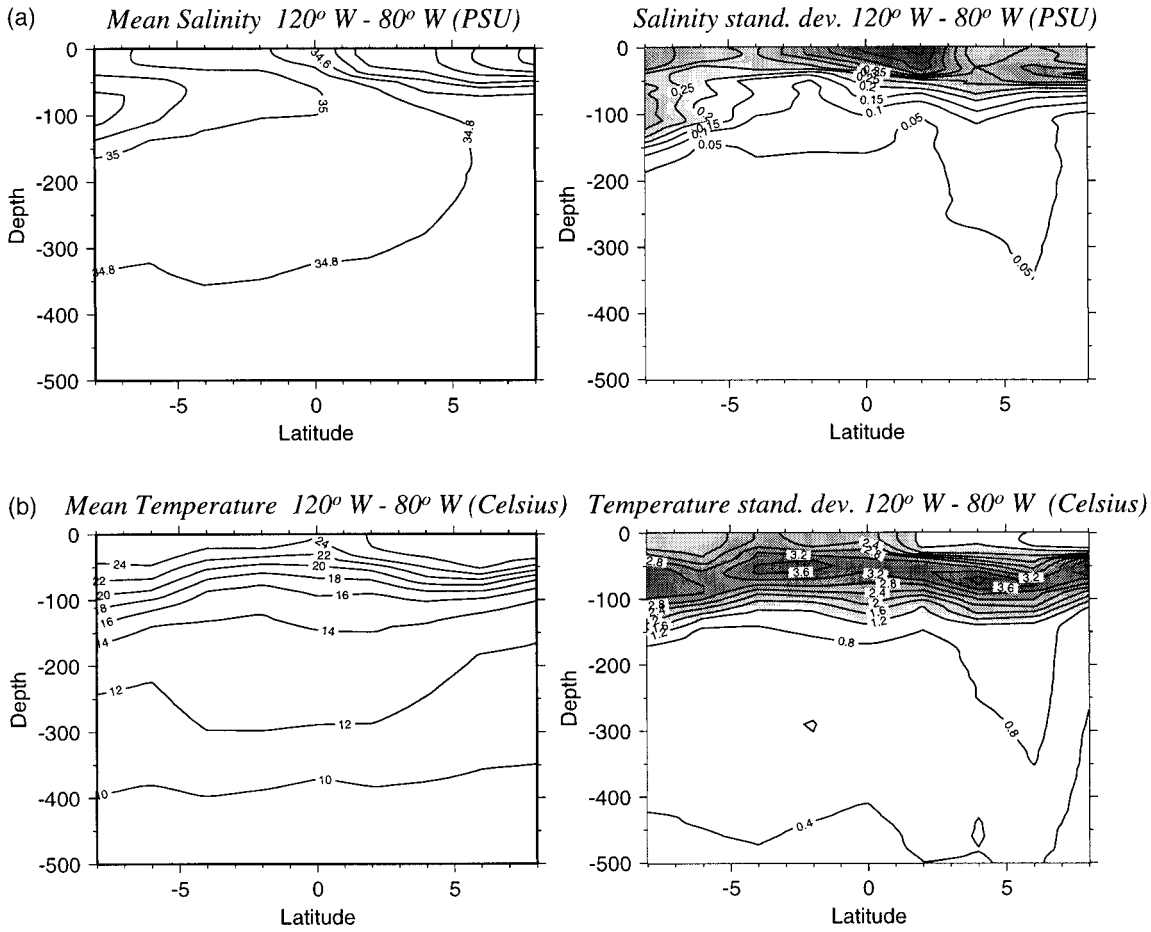

FIG. 4. (a) Salinity mean and standard deviation and (b) temperature. As in Fig. 2, but for the eastern Pacific (80°–120°W).

The variability of the high salinity waters in the thermocline has been studied extensively during the Tropical Ocean Global Atmosphere Coupled Ocean–Atmosphere Response Experiment (TOGA COARE) (Webster and Lukas 1992). Studies within the TOGA COARE framework of observations confirm the existence of a meridional salinity gradient barrier to the northward extension of the high salinity Tropical Water (Gouriou and Toole 1993), which migrates meridionally (Huyer et al. 1997). In places where a strong salinity gradient is present (e.g., in a barrier layer, near the subsurface salinity maximum) salinity variability is often unrelated to temperature variability. For this reason, it is expected that salinity estimates based on T–S relations will not capture all salinity variability in the isothermal layer and at depths below the mixed layer.

In the central Pacific (Fig. 3), the mean surface salinity is higher in the Southern than in the Northern Hemisphere. The mean salinity maximum is positioned at the mean depth of the thermocline between the 100- and 200-m depth. The mean thermocline is shallower than farther west (Fig. 2).

At the surface in the Southern Hemisphere, under the Southern Pacific Convergence Zone, the salinity standard deviation is relatively high compared to the low standard deviation at the equatorial surface (Delcroix et al. 1996). North of 6°S, the maximum of salinity standard deviation is not located at the surface; rather it is at the depth of the subsurface salinity tongue. This is also the mean depth of the thermocline in this region and the depth of highest temperature variance. The salinity variability in this region is attributed to different causes, which can be specified using the formalism of Bindoff and McDougall (1994). They describe the dynamics in terms of three processes: ''pure freshening,'' ''pure warming,'' and ''heave.'' Part of the salinity variability depends on heave and is related to vertical displacements of the pycnocline. In the case of pure freshening, however, the behavior of the halocline may be independent of the thermocline. An example of pure freshening is the horizontal advection of the subsurface salinity tongue, as described by Donguy (1994). This is associated with a temporal variability in the T–S relation, which will not be captured in a T–S salinity estimate.

In the eastern Pacific (Fig. 4), the mean thermocline

is most shallow, and the mean subsurface salinity maximum is located south of the domain depicted. This is also the case for the mean surface salinity maximum. In the mean salinity field, the surface salinity is low north of the equator and is strongly stratified around the 50-m depth (see also Lukas 1986). This is approximately the mean depth of the thermocline in the eastern tropical Pacific.

When comparing the standard deviations for the central Pacific (Fig. 3) to the western (Fig. 2) and the eastern Pacific (Fig. 4), the salinity variability in the mixed layer in the central Pacific is low. With the absence of a barrier layer, and the relatively low variability in precipitation and evaporation in the central Pacific, the estimates in this region are expected to give a relatively accurate salinity representation for the mixed layer.

Salinity variability in the eastern Pacific has several possible causes. Part of the variability may be due to evaporation and precipitation (E–P) balances affected by the displacements of the Intertropical Convergence Zone, while part may be due to the fluctuations of the zonal current in the eastern Pacific just north of the equator (Wooster 1969). Surfacing of the (relatively salty) Equatorial Undercurrent also contributes to salinity variability in this region (Lukas 1986). Comparing the standard deviation for salinity and temperature, the salinity variability in the surface layer seems disconnected from the temperature variability. A climatological T–S relation might therefore not be applicable in this region. Below the surface layer, salinity and temperature have very low variance. Hence, the use of a T–S relation at lower depth is not likely to cause significant errors in the eastern Pacific.

3. Procedure

Despite the specific problems identified in the previous section, we can obtain a useful salinity estimate from the climatological T–S relationship, especially when combined with SSS observations. Various methods have been developed to combine T–S salinity estimates with SSS observations. In this paper, a new method is developed to improve these estimates with the use of sea level observations.

The method for salinity estimation and correction is developed with measured profiles of $S(z)$ and $T(z)$, SSS, and dynamic heights relative to 500 m from CTD measurements of Ando and McPhaden (1997). The depth of 500 m was chosen as a reference level because many of the CTDs terminate at this level. The choice for 500 m as a reference level for the computation of dynamic height implies a loss of approximately 5%–15% of the sea level signal (Busalacchi et al. 1994). For dynamic height discrepancies of the order of 5–8 cm, this part of the signal will remain below 1 dyn cm.

The procedure for salinity estimation and correction is done in two steps while holding back the observed salinity profile, $S_{obs}(z)$. In the first step, salinity will be generated using $T(z)$ and T–S, applying different methods to combine the estimates with SSS. The resulting profiles will be called the estimated salinity, $S_{est}(z)$. One of the salinity estimation methods will then be selected and applied. In the next step the estimates will be corrected on the basis of dynamic height differences between the dynamic height computed from $T(z)$ and $S_{obs}(z)$, DH_{obs}, and the dynamic height computed from $T(z)$ and $S_{est}(z)$, DH_{est}. The corrected salinity profiles will be called $S_{cor}(z)$.

TABLE 1. Summary of abbreviations.

Abbreviation	Meaning
$T(z)$	Observed temperature
$S_{obs}(z)$	Observed salinity
$S_{est}(z)$	Estimated salinity, T–S or T–S and SSS
$S_{cor}(z)$	Corrected salinity, dynamic height plus estimated
DH_{obs}	Dynamic height computed from $T(z)$ and S_{obs}
DH_{est}	Dynamic height computed from $T(z)$ and S_{est}
DH_{cor}	Dynamic height computed from $T(z)$ and S_{cor}

The salinity estimation and correction method is developed using only part of the CTD dataset (1979–89), the dependent part, and then tested using the CTD dataset for (1990–96), the independent part. The testing of the method will be done by comparison to the salinity profiles $S_{obs}(z)$ that were held back in the salinity estimation. This will give a verification of both the salinity estimation and correction method. In addition, the dynamic height computed with $T(z)$, S_{cor}, and DH_{cor} will be compared with DH_{obs}. Next, the effect of observational errors on the salinity estimates will be investigated. A summary of the abbreviations used in this paper is given in Table 1.

4. The salinity estimate with T–S and SSS

The first step in the estimation of salinity is the use of climatological T–S relations (Levitus and Boyer 1994; Levitus et al. 1994). This estimate can be combined with SSS observations. In this section, four different methods to estimate salinity will be presented and compared. In three of these methods, SSS, assumed to be known from observations, is combined with T–S.

The use of SSS is restricted to the isothermal layer. The bottom of the isothermal layer is defined as the depth at which the temperature is 0.5°C below the sea surface temperature, according to the 0.5°C criterion often used in observational studies of the mixed layer (e.g., Sprintall and Tomczak 1992).

After a description of the methods, we will give an example of the use of the methods for a profile in the western Pacific. In section 4b, the resulting salinity estimates are evaluated, and from the different estimation methods one method is selected for use in the correction procedure.

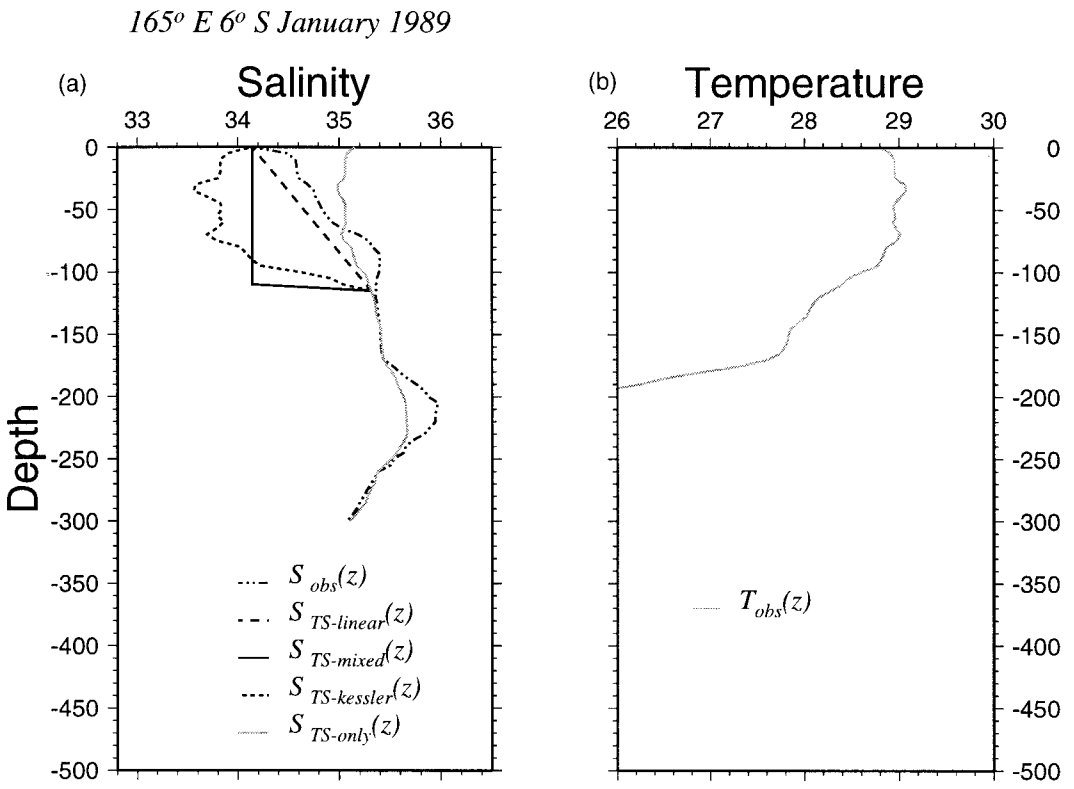

FIG. 5. (a) CTD profile in Jan 1989 at 6°S, 165°E. The dash-double-dot line shows the observed salinity (S_{obs}), whereas the continuous line gives the salinity from the climatological T–S curve (TS-only). Linear interpolation from the salinity at the bottom of the mixed layer to SSS (TS-linear) is depicted with a long-dashed line. Constant salinity in the mixed layer (TS-mixed) is given by the light colored continuous line, and linear interpolation of the T–S curve in the mixed layer (TS-Kessler) is presented by the dotted line. (b) The temperature profile reveals the temperature inversion.

a. Four methods to estimate salinity

The different salinity estimation methods are as follows.

- TS-only: The simplest way to produce a salinity estimate involves conversion of $T(z)$ to $S_{est}(z)$ on the basis of climatological T–S relationships that depend on the location in the Pacific. The next three methods differ in the way the isothermal layer is handled.
- TS-mixed: This estimate assumes a constant salinity equal to observed SSS throughout the isothermal mixed layer.
- TS-linear: In this approach, salinity changes linearly from the estimated value at the depth of the isothermal layer to the observed salinity value at the surface.
- TS-Kessler: Donguy et al. (1986) and Kessler and Taft (1987) suggest linear interpolation on T–S coordinates from the T–S derived S and T at the base of the isothermal layer to S and T at the surface.

Before these four methods are evaluated for the entire CTD dataset, the methods will first be illustrated in the profile of Fig. 5, which is located in the western Pacific south of the equator. In this particular case, the isothermal layer is not the same as the mixed layer because a barrier layer is present. Figure 5 demonstrates how the barrier layer complicates the T–S salinity estimation in the mixed layer. In this profile, the salinity in the isothermal layer is highly stratified, so the assumption that salinity remains constant is not valid. Consequently, the TS-mixed salinity estimate strongly deviates from the observed values. The TS-Kessler estimate generates some stratification in the mixed layer but does not correctly capture the stratification in the observations (Fig. 5a). The salinity misestimation is a result of the inversion in the mixed layer temperature, which is shown in a temperature–depth profile in Fig. 5b. The temperature inversion, although smaller than half a degree Celsius, is enough to spoil the TS-Kessler estimate. In fact, as shown in Fig. 6, the linear interpolated line on T–S coordinates between T and S at the bottom of the isothermal layer and T and S at the surface needs to be extrapolated to obtain a salinity value for the temperature maximum in the inversion. This temperature inversion is not an incidental phenomenon, as shown by Vialard and Delecluse (1998a). Based on an analysis of 1512 CTD profiles in the COARE region, they conclude that a temperature inversion in the barrier layer is an average characteristic of the western Pacific. Consequently, TS-Kessler may not work satisfactorily in regions where a barrier layer is present. The sensitivity of TS-Kessler for temperature inversions is a drawback

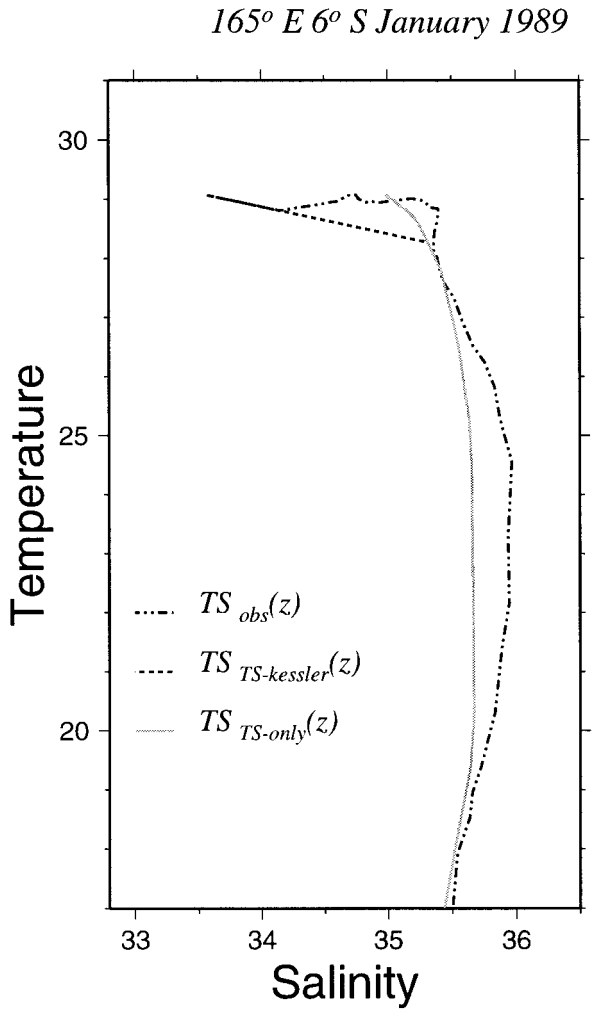

FIG. 6. Temperature vs salinity in a CTD profile in Jan 1989 at 6°S, 165°E. The TS-Kessler and TS-only salinity estimates are demonstrated with line types as in Fig. 5.

of this method. However, while both TS-Kessler and TS-mixed have errors in case of a strong salinity stratification, the TS-linear estimate is relatively close to the observations.

b. Evaluation of salinity estimation errors

To determine which of the four salinity estimation methods described above is most suitable for our objective, we evaluate profiles in data-rich areas. Good time sampling of the salinity field by the CTD profiles is available for meridional cross sections at 165°E and 110°W. Along these cross sections the salinity is estimated with the use of the temperature observations and T–S relationships to quantify the errors made in salinity estimation with each of the four methods. The root-mean-square (rms) difference between estimated and observed salinity, the rms salinity estimation error, is given for every latitude and depth along these cross

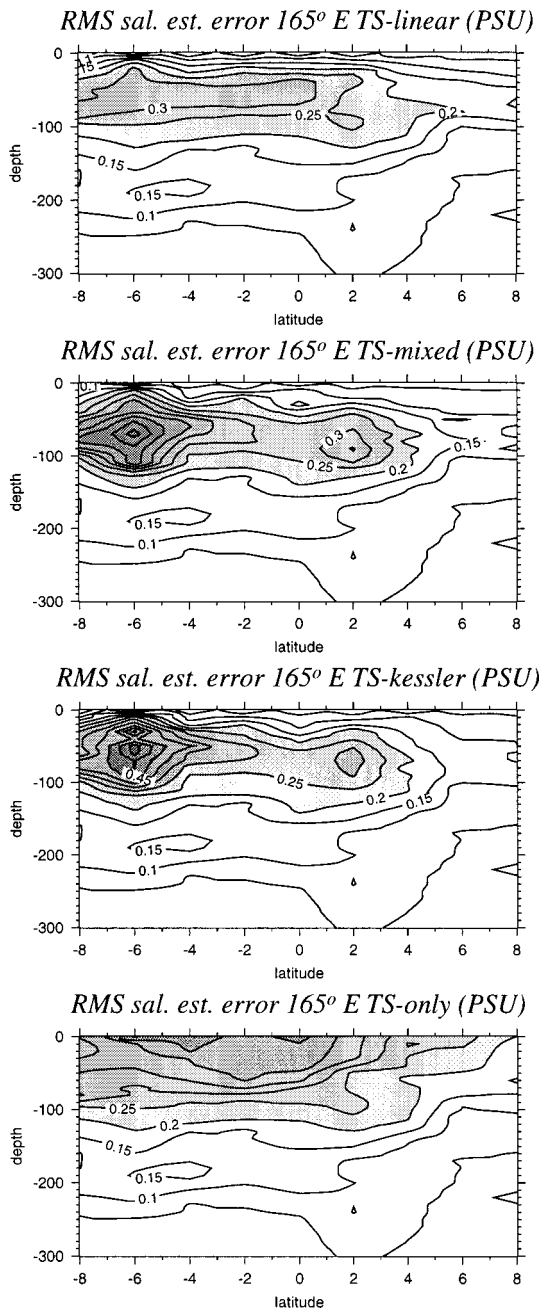

FIG. 7. Depth–latitude cross sections along 165°E: the rms difference between salinity as estimated by each of the four T–S estimation methods and observed salinity, applied on the CTDs for the period 1979–89. TS-linear: linear interpolation salinity from depth of isothermal layer to surface. TS-mixed: constant salinity from depth of isothermal layer to surface. TS-Kessler: linear interpolation T–S relation from depth isothermal layer to surface. TS-only: just the climatological relation. The rms values greater than 0.2 psu are shaded. Contour interval is 0.05 psu.

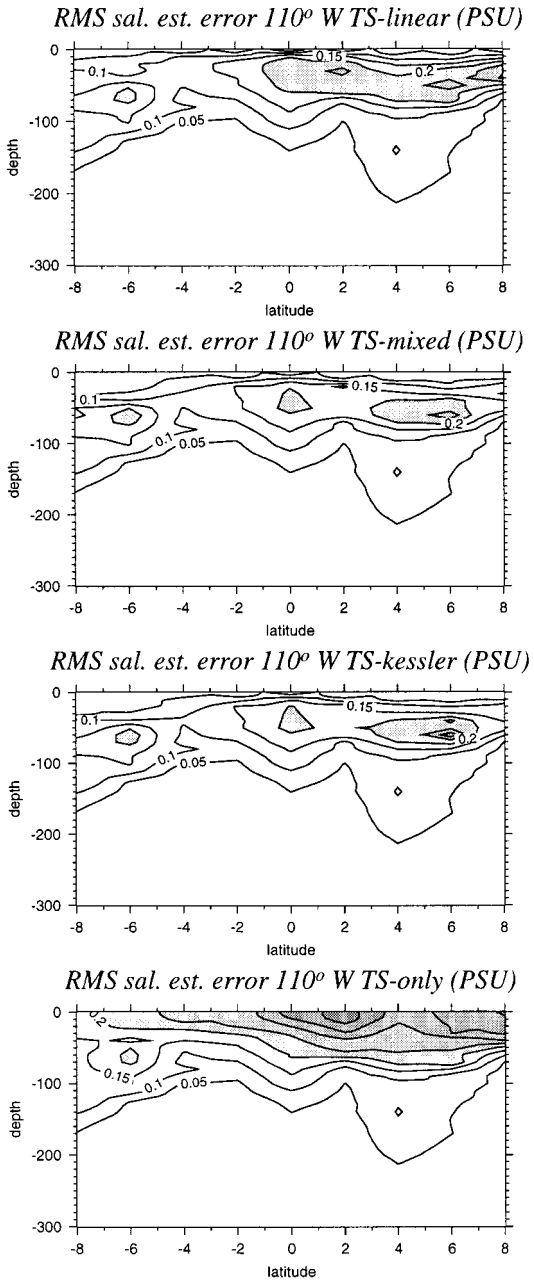

FIG. 8. Depth–latitude cross sections along 110°W: rms difference between salinity as estimated by each of the four T–S estimation methods and observed salinity. As in Fig. 7.

sections in Figs. 7 and 8. The selection of the salinity estimation method will be based on the rms salinity estimation error as determined for the 1979–89 CTD dataset, the dependent dataset. Thus, the selection of the salinity estimation will be independent of the dataset that is used for verification.

In the meridional cross section along 165°E (Fig. 7), the estimation errors are largest for the mixed layer, as was anticipated based on Fig. 2. Use of a climatological T–S relation, without SSS observations (TS-only), results in a typical rms estimation error of 0.4 psu for the upper ocean in the equatorial region. The use of SSS observations in TS-linear reduces the rms values to a level of 0.3 psu. Both TS-mixed and TS-Kessler significantly improve the salinity estimation north of the equator but fail to do so between 2° and 9°S. Inspection of individual profiles shows that the errors at this location are related to the inability of the methods to simulate a realistic stratification in presence of a barrier layer. The shortcomings of TS-Kessler and TS-mixed, as shown by the bull's-eyes in Fig. 7, are not evident in the more homogeneous rms error field for TS-linear.

Along 110°W (Fig. 8), the salinity estimate based on TS-only is relatively good, as compared to TS-only estimates at other longitudes (not shown). Still, some errors are made north of the equator, as was expected from the high salinity variability in this region (Fig. 4). Comparing the three different methods that utilize SSS, TS-mixed and TS-Kessler are most successful in reducing the salinity estimation error for this cross section. The TS-linear method produces slightly higher errors, but the rms value does not exceed 0.25 psu. In general, salinity estimation in the eastern Pacific benefits from the use of SSS observations.

Based on the rms salinity estimation errors for the cross sections at 110°W, TS-mixed and TS-Kessler seem the most useful of the methods described. Along the 165°E section, however, these methods generate considerable estimation errors. Since the salinity variability in the western Pacific is relatively high, we want to specifically minimize the errors in that region. Figure 7 shows that in the western Pacific, the use of SSS in TS-mixed and TS-Kessler generates larger rms salinity estimation errors than when no SSS is used. Although TS-linear does not always give the best estimate, this method produces a better estimate than TS-only for all profiles analyzed. This is not always the case with TS-Kessler and TS-mixed (Fig. 5). Therefore, TS-linear is selected as the model for combination of T–S and SSS in salinity estimation in the following section.

It is demonstrated with the analysis of these four methods that the salinity estimate still contains errors, no matter which of the four methods is used. In the next section, we will investigate the use of dynamic height information to reduce these errors.

5. Use of dynamic height to improve the salinity estimate

As section 4 shows, the TS-linear method does not work perfectly because it ignores temporal variations in the subsurface T–S relation and sometimes misestimates salinity in the isothermal layer. Consequently, dynamic height computed from $T(z)$ and $S_{est}(z)$, DH_{est}, will deviate from DH_{obs}, computed from $T(z)$ and $S_{obs}(z)$. For example, a uniform error of 0.5 psu over the top 130 m in the Tropics leads to an error near 5 dyn cm. In

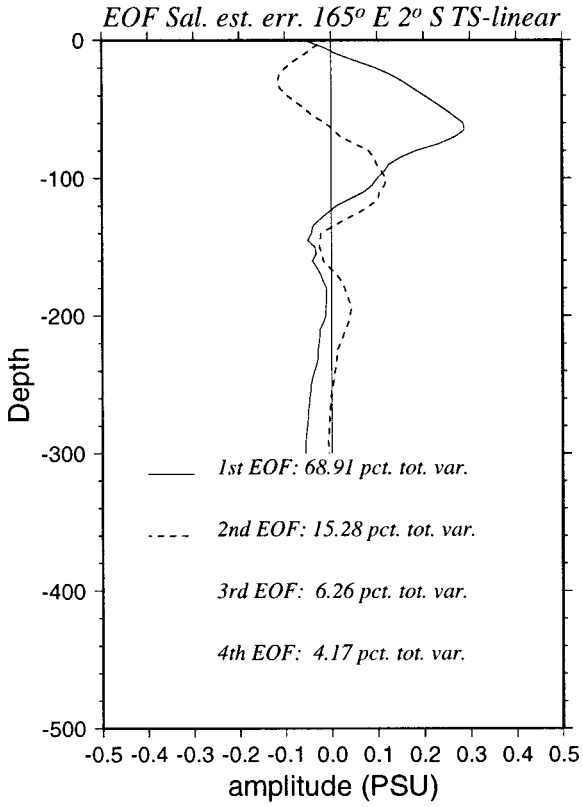

FIG. 9. EOF analysis for the TS-linear salinity estimate at 2°S, 165°E. The variance explained by the first four EOFs is denoted in the figure.

this section, dynamic height discrepancies will be translated into a salinity correction.

Dynamic height differences between DH_{obs} and DH_{est} only provide information on the salinity misestimation and not on the entire salinity signal. Therefore, the dynamic height information is used to correct the estimated salinity by adding a correction profile, $\delta S(z)$, to $S_{est}(z)$. The correction profile is determined with the aid of statistical information on the salinity estimation errors from the dataset for 1979–89. The method will later be tested with the independent dataset from the 1990–96 period.

To determine the vertical structure of the salinity correction, the salinity estimated from TS-linear was compared to salinity observations. The salinity estimation errors ($S_{est} - S_{obs}$) for 1979–89 were separately grouped in bins of 2° latitude and 10° longitude. An empirical orthogonal function (EOF) analysis was then performed on those bins with more than 15 profiles. EOFs could be determined for 35% of the bins in the tropical Pacific.

An example of the first two EOFs for the salinity estimation error are given in Fig. 9. At all bin locations, the first EOFs display a maximum amplitude at the top of the thermocline. Because the salinity estimation error is zero by definition at the surface, the absolute amplitude of the EOF tends to decrease from the bottom of the isothermal layer to the surface. In regions where the CTD sampling is regular in time, the principal components associated with the first EOF explain 60%–80% of the total variance. The significance of the EOFs was tested by the method of North et al. (1982). For most of the profiles, only the first two EOFs are significant. For the remainder, only the first EOF is significant.

For the discussion that follows we decided to limit ourselves to using only one EOF. This was done because the first EOF accounts for most of the variance and because the use of only one EOF would be very conservative and limit any chance of instability in the fit. One of the reviewers of an earlier draft suggested that two EOFs be used. A test with this setup caused problems that will be discussed at the end of this section.

Suppose the temperature profile $T(z)$, the sea surface salinity SSS, and the dynamic height DH_{obs} are known within a certain accuracy at a given location. The salinity can now be estimated with the use of the dynamic height difference and a correction function following a two-step procedure.

Step 1: A salinity estimate $S_{est}(z)$ is made applying the TS-linear method with $T(z)$, T–S, and SSS. As a result of the salinity estimation errors, DH_{est} will deviate from the DH_{obs}.

Step 2: The salinity estimation errors are corrected with the correction function $\delta S(z)$, which is determined by the first EOF of the salinity estimation error, EOF(z), multiplied by an empirical weighting factor, f, and scaled by the dynamic height difference ($DH_{obs} - DH_{est}$). The corrected salinity $S_{cor}(z)$ is defined as follows:

$$S_{cor}(z) = S_{est}(z) + \delta S(z) \quad (1)$$

with

$$\delta S(z) = f \times (DH_{est} - DH_{obs})\ EOF(z). \quad (2)$$

[The method of Cressman (1959) was used to interpolate EOF values over grid values without data.]

The optimal values for the factor f were determined with the use of the CTDs from the 1980s through iterative minimization of the dynamic height difference. The resulting optimal f, f_{opt}, is a function of longitude and latitude and has values in the range from 80 to 120 m^{-1}. To test the effect of the choice of f on the solution, the 1980 CTDs were corrected for different values of f. The correction was applied with the spatially dependent f, and fixed values of $f = 80$ and $f = 120$. Differences between $f = 80$ and the spatially dependent f were lower than 0.02 psu. For the salinity correction in this section we use a constant f value to keep the method as simple as possible. The value we chose for f is 80, which is on the conservative side and avoids overfitting the salinity profile.

One of our reviewers suggested a detailed method using two rather than one EOF. In this method, the TS-only method was used to generate the two EOFs. The selection of the two EOFs was obtained by a minimization with a constraint of both dynamic height and SSS. When this method was tested, we found that there were

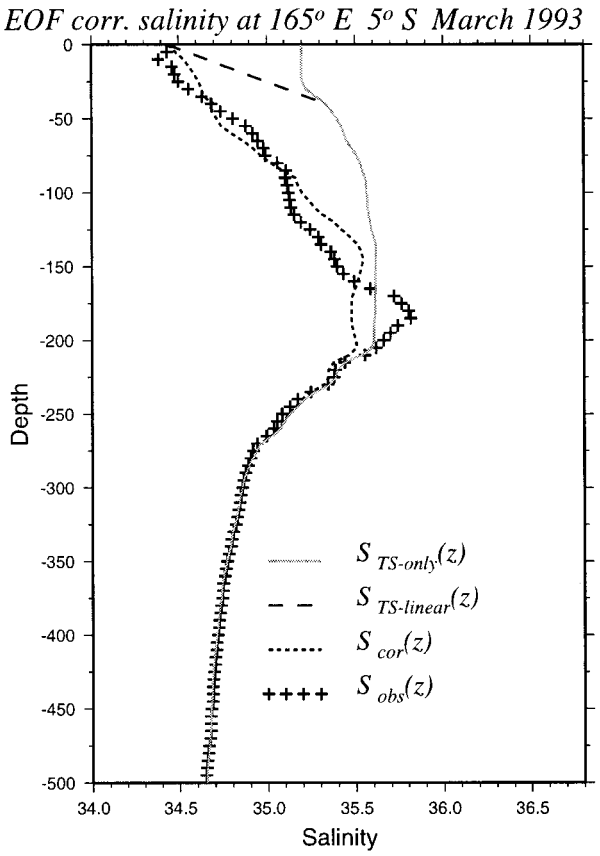

FIG. 10. Salinity correction with the use of dynamic height difference and the first EOF of the salinity estimation error using TS-linear. The method is demonstrated with the use of a CTD profile at 5°S, 165°E in Mar 1993. The profile for $S_{est}(z)$ from TS-only is also shown for comparison.

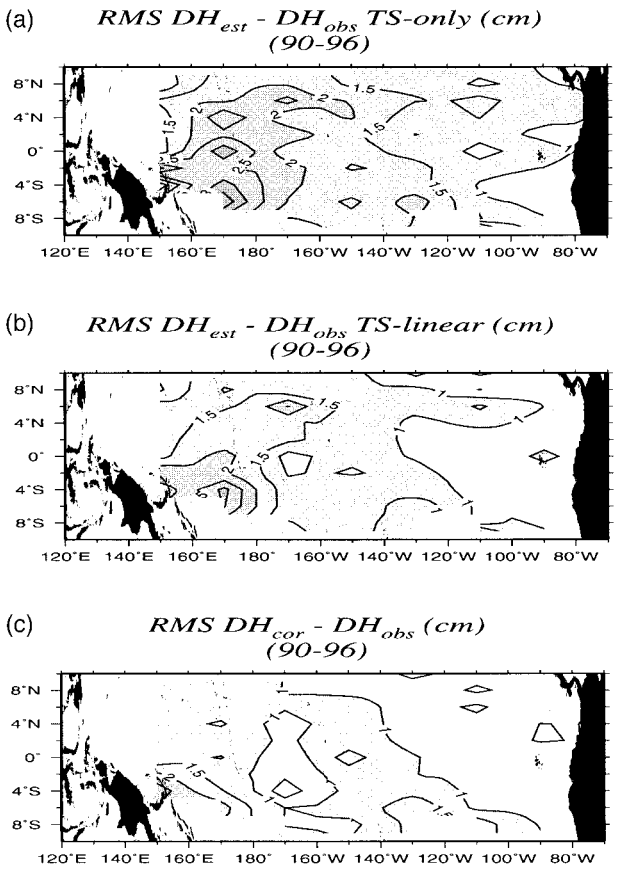

FIG. 11. (a) The rms of the dynamic height estimation error when salinity is estimated with the TS-only. (b) Same, but for TS-linear. (c) The rms dynamic height estimation error after EOF correction of the TS-linear salinity estimate. Analysis is based on CTD data from 1990–96.

improvements in the salinity profiles in some cases. However, in other cases, the two EOFs interacted with each other to result in spurious maxima along the profile in which the absolute difference between the observed and fitted profiles exceeded 1 psu. Since there is no constraint on $S(z)$ below the surface and the second TS-only EOF has two maximums, the two EOF method is not very stable. As a consequence, our original method using only one EOF actually performed better overall and has been retained here.

6. Testing of the results with independent CTD data

The results of the previous section will be verified with an independent CTD dataset in this section. For all profiles in the 1990–96 period, the salinity estimates S_{est} are generated with T–S and SSS using the TS-linear method. The resulting estimates are corrected using (1) and (2), where $f = 80$ in (2) is based on the analysis of the 1979–89 dataset, as described in section 5.

An example is presented for the independent dataset in Fig. 10. For this profile in 1993, the salinity estimate is remarkably improved with the EOF correction method. The difference in dynamic height, for this profile 4.0 dyn cm, is a result of overestimation of salinity. After correction of the salinity estimate, the resulting dynamic height difference ($DH_{cor} - DH_{obs}$) is 1 dyn cm.

Also in other regions of the tropical Pacific the salinity estimation and correction method works successfully. The results are presented in Fig. 11 along with the errors for TS-only. The rms differences between DH_{est} and DH_{obs} are lower for TS-linear than for TS-only, indicating that the use of SSS improves the salinity estimate. Figure 11 shows that this is not only the case for the western Pacific, where salinity variability is high, but also for the central and eastern Pacific. The rms values of the dynamic height differences are further reduced by 0.5 dyn cm by the correction in dynamic height. This reduces the difference between DH_{cor} and DH_{obs} to roughly 1 dyn cm. The reduction of the rms dynamic height differences is largest in the western Pacific, where salinity misestimation has the largest effect on the dynamic height.

Figure 12 shows the rms $S(z)$ errors along 165°E. The

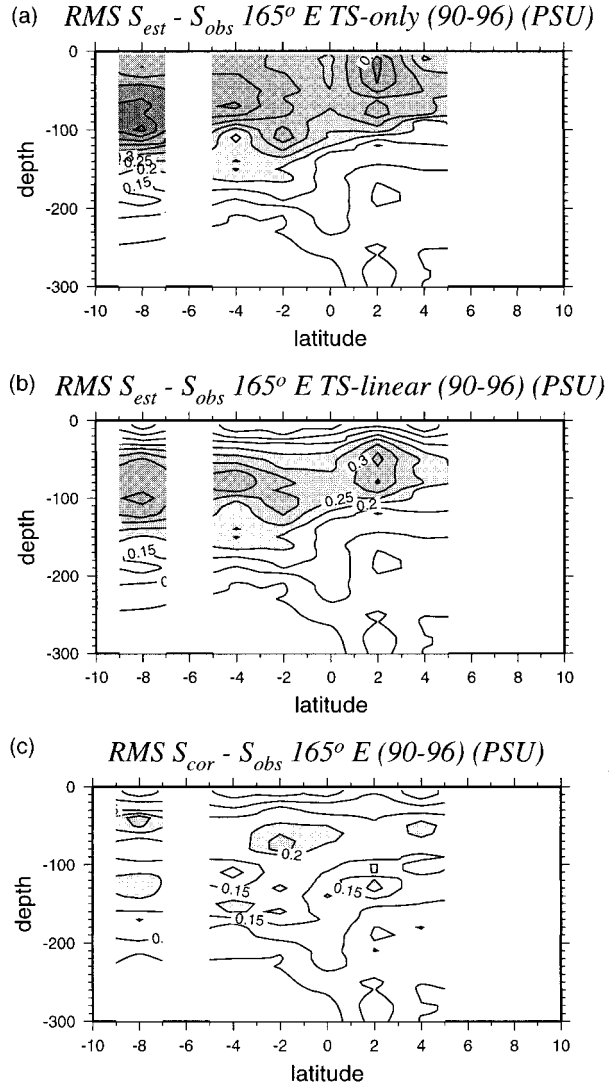

FIG. 12. The rms of the salinity estimation error along 165°E, as determined from the independent CTD dataset (1990–96). (a) The rms difference TS-only salinity estimate and observed salinity. (b) The rms difference TS-linear estimate and observed salinity. (c) The rms difference between the corrected and observed salinity. The corrected salinity is computed from TS-linear (see text). Contour interval is 0.05 psu. The rms values greater than 0.2 psu are shaded. Regions where less than five profiles were available for this period are not shown.

figure shows how the salinity estimation is improved from TS-only by the use of SSS and further improved by the EOF correction technique. The combination of T–S salinity estimates with SSS observations reduces the rms salinity estimation error in the upper ocean from 0.35 psu to below 0.2 psu. The maximum rms difference between $S_{\text{est}}(z)$ and $S_{\text{obs}}(z)$ is 0.55 psu for TS-only and 0.42 psu for TS-linear. Using the EOF correction, the maximum rms value for the difference between $S_{\text{cor}}(z)$ and $S_{\text{obs}}(z)$ is only 0.22 psu. Tests with the independent CTD dataset at 170° and 110°W show that the correction method also improves salinity estimates in other regions than the western Pacific, although salinity error reductions are not as large as is the case for the 165°E cross section.

The verification of the salinity estimation and correction methods with the independent CTD dataset gives positive results. Not only is the difference between DH_{est} and DH_{obs} for TS-linear lower than for TS-only, the DH_{cor} is noticeably closer to DH_{obs} than DH_{est} for either of the salinity estimation methods. The improvement in dynamic height computation is associated with an improvement in the determination of $S(z)$.

To test the robustness of the salinity correction method, we partitioned the CTD dataset in a subset with positive Southern Oscillation Index (SOI+) and a subset with a negative index (SOI−). For both the SOI+ and the SOI− profiles the EOFs of the salinity estimation error were determined. The resulting EOFs look very similar to the first EOF that has been determined for the 1979–89 dataset. As a test, the first EOF for the SOI− subset is used in the dynamic height correction of all SOI+ profiles. The reduction of salinity estimation errors with this SOI− profile is equally effective as with the first EOF for the 1979–89 dataset. This suggests that even when ENSO variability is eliminated from the dataset, the salinity estimation error has characteristics that can be modeled with the profile of the first EOF.

The success of the estimation and correction method is partly related to the seasonal and interannual information that is contained in the SSS and DH observations, but that is absent from the T–S climatology. As a consequence, the method is very helpful in the reconstruction of salinity variations related to ENSO.

To test the sensitivity of the methods to observational noise, we modified the observed dynamic height [$\text{DH}(T_{\text{obs}}, S_{\text{obs}})$] by adding white noise to represent observational errors. The correction has been performed with two different noise levels: white noise with a 1 dyn cm rms, and white noise with a 2 dyn cm rms. The reconstruction of the ''true'' dynamic height with these erroneous observations is reasonably good. However, the reconstruction of the salinity is clearly affected by the observational noise in dynamic height. The salinity estimation error remains below the 0.3 psu when the noise is at a 1-cm level. This is still lower than TS-linear salinity estimation errors. When altimetric noise has an rms value of 2 cm, the salinity estimation errors increase but remain below 0.35 psu. This is a salinity error comparable to the TS-linear estimation error. In reality, $T(z)$ is also not known perfectly. Consequently, actual errors in the TS-linear salinity will be larger than assumed thus far. Although the observational errors of the sea level may affect the salinity estimate, we conclude that the benefits of using these data outweigh the risks, when the altimetric noise remains at or below the 2-cm rms level. In addition, it is very likely that observational errors will be filtered out by the assimilation scheme.

7. Discussion

With the TOGA–Tropical Atmosphere Ocean array, numerous scientific cruises, and expendable bathythermograph observations from Voluntary Ships of Opportunity, the temperature in the equatorial Pacific is well monitored. The available temperature data are widely used for data assimilation purposes. At NCEP, the temperature assimilation has improved temperature analysis and model initialization. Model salinity, however, could benefit from data assimilation. Unfortunately, salinity data are sparse, and their time and space sampling highly irregular. As an alternative approach, salinity variability can be derived from sea level observations at locations where temperature is well known.

In this study, salinity profiles are generated in a two-step procedure. First, the salinity is estimated with the use of T–S relations and SSS. Second, the salinity estimate is corrected with the use of dynamic height information. The CTD dataset from Ando and McPhaden (1997) is used to develop and evaluate the salinity estimation and correction methods. The dependent part of the dataset is used to select a salinity estimation method and develop the correction technique, while the independent dataset is used to test the results.

Four different methods to estimate salinity are evaluated with a CTD dataset for 1979–89. Three of these methods combine a T–S relationship with sea surface salinity observations. The fourth method, TS-only, uses only T–S to estimate salinity. By holding back the salinity observations, $S_{obs}(z)$, and estimating salinity with $T(z)$, T–S, and SSS, the different salinity estimation methods are evaluated. Our preferred method to estimate salinity in the tropical Pacific is the method denoted by TS-linear, a linear interpolation of salinity from the bottom of the isothermal layer to the surface. This method gave good results in the western Pacific and did not generate severe errors in the central and eastern Pacific. Of course, alternative methods may lead to better results. To keep the method simple, we limited our evaluation to the four methods described in section 4.

The salinity estimates based on the TS-linear method [$S_{est}(z)$] can be corrected with the use of dynamic height information. Dynamic height computed from $T(z)$ and $S_{est(z)}(z)$ is compared to dynamic height from $T(z)$ and $S_{obs}(z)$. The difference is used to scale the salinity correction. The vertical profile for the salinity correction is based on an EOF analysis of the salinity estimation errors.

The rms differences between dynamic height computed with $T(z)$ and T–S estimates of salinity and dynamic height computed with $T(z)$ and observed salinity ($DH_{est} - DH_{obs}$) are reduced when the estimate is combined with SSS. The remaining difference between the dynamic height computed with $T(z)$ and the corrected salinity, DH_{cor}, and DH_{obs} has an rms value of roughly 1 dyn cm.

The reduction in dynamic height difference through the use of SSS and dynamic height differences is associated with a reduction in salinity estimation errors. For example, the use of SSS reduces the difference between $S_{est}(z)$ and $S_{obs}(z)$ by 0.1 psu in the western Pacific, while the correction based on addition of the dynamic height difference results in a further reduction of the difference between $S_{cor}(z)$ and $S_{obs}(z)$ by 0.2 psu. In general, the salinity estimation errors are reduced by a factor of 2 by combination with SSS and further corrected with dynamic height information. Results with the independent dataset agree with the results from the dependent dataset.

It is a challenging idea to use altimetry for the correction technique described above. With altimetric sea level variability reaching 2-cm accuracy (Cheney et al. 1994), the T/P dataset should be able to improve model dynamics through the correction of the salinity field. If simultaneous altimetric sea level observations were available for every CTD profile, the salinity correction method described above could be directly tested with altimeter data. Unfortunately, such a synchronous dataset is not available, and direct testing with CTDs and altimetry is hardly possible. To simulate the use of altimetric observations, we applied the method to pseudo observations that were generated by adding white noise to the DH_{obs} estimates. When altimetric noise remains at or below the 2-cm rms level, the correction with dynamic height still improves the salinity estimate. In an OGCM, simulated temperature and salinity can be combined with sea level observations, applying the methods described above through data assimilation.

The assimilation of sea level data in an OGCM is not straightforward. In assimilation schemes that are based on correction of prognostic variables, such as the technique currently used at NCEP, the altimetric sea level deviation must be translated into a subsurface correction (Behringer et al. 1998; Cooper and Haines 1996; De Mey and Robinson 1987). Other methods, like Kalman filtering or smoothing (e.g., Miller et al. 1995), and the four-dimensional variational (4D-Var) technique (e.g., Thépaut and Courtier 1991) do not necessarily require such a translation. These techniques, however, require much more computer time for the assimilation than the three-dimensional variational technique used at NCEP (for details on this technique, see Derber and Rosati 1989).

For the NCEP ocean model, Behringer et al. (1998) developed a technique in which the altimeter observations are used to correct the temperature. According to the experiments by Cooper (1988), this correction of temperature without updating salinity is not complete and may introduce unrealistic velocity fields. In the western Pacific the effect of salinity variability on density and hence velocity is too large to be neglected.

It is therefore suggested that the assimilation scheme uses altimeter data to correct both temperature and salinity. At the moment, this is being tested in an OGCM assimilation scheme, which takes into consideration the

difference between dynamic height deviations due to salinity differences and the sea level estimates from T/P.

Acknowledgments. The authors are indebted to K. Ando and Mike McPhaden for providing the CTD dataset. Billy Kessler kindly provided his salinity estimation method. The authors wish to thank Ming Ji, Ants Leetmaa, and Dave Behringer for many useful discussions. The help of Bob Cheney is greatly appreciated. Christophe Maes and Gerrit Burgers provided useful suggestions for the manuscript. The suggestions of Roger Lukas were of great help to improve the manuscript. Three anonymous reviewers are acknowledged for their fruitful comments. Femke Vossepoel's visit to the Washington, D.C., area was partly funded by a Fulbright scholarship and the Netherlands Fulbright Alumni Association Award. Her Ph.D. project is funded by the Space Research Organization Netherlands, SRON EO-024.

REFERENCES

Anderson, S. P., R. A. Weller, and R. B. Lukas, 1996: Surface buoyancy forcing and the mixed layer of the western Pacific warm pool: Observations and 1D model results. *J. Climate,* **9,** 3056–3085.

Ando, K., and M. J. McPhaden, 1997: Variability of surface layer hydrography in the tropical Pacific Ocean. *J. Geophys. Res.,* **102,** 23 063–23 078.

Behringer, D. W., M. Ji, and A. Leetmaa, 1998: An improved coupled model for ENSO prediction and implications for ocean initialization. Part I: The ocean data assimilation system. *Mon. Wea. Rev.,* **126,** 1013–1021.

Bindoff, N. L., and T. J. McDougall, 1994: Diagnosing climate change and ocean ventilation using hydrographic data. *J. Phys. Oceanogr.,* **24,** 1137–1152.

Busalacchi, A. J., M. J. McPhaden, and J. Picaut, 1994: Variability in the equatorial Pacific during the verification phase of TOPEX/POSEIDON mission. *J. Geophys. Res.,* **99** (C12), 24 725–24 738.

Cheney, R. E., L. Miller, R. Agreen, N. Doyle, and J. Lillibridge, 1994: TOPEX/POSEIDON: The 2-cm solution. *J. Geophys. Res.,* **99** (C12), 24 555–24 564.

Cooper, M., and K. Haines, 1996: Altimetric assimilation with water property conservation. *J. Geophys. Res.,* **101** (C1), 1059–1077.

Cooper, N. S., 1988: The effect of salinity in tropical ocean models. *J. Phys. Oceanogr.,* **18,** 697–707.

Cressman, G. P., 1959: An operational objective analysis system. *Mon. Wea. Rev.,* **87,** 367–374.

Delcroix, T., G. Eldin, and C. Hénin, 1987: Upper ocean water masses and transports in the western tropical Pacific. *J. Phys. Oceanogr.,* **17,** 2248–2263.

——, C. Hénin, V. Porte, and P. Arkin, 1996: Precipitation and sea-surface salinity in the tropical Pacific Ocean. *Deep-Sea Res.,* **43** (7), 1123–1141.

De Mey, P., and A. Robinson, 1987: Assimilation of altimeter eddy fields in a limited-area quasigeostrophic model. *J. Phys. Oceanogr.,* **17,** 2280–2293.

Derber, J., and A. Rosati, 1989: A global oceanic data assimilation system. *J. Phys. Oceanogr.,* **19,** 1333–1347.

Donguy, J.-R., 1994: Surface and subsurface salinity in the tropical Pacific Ocean. *Progress in Oceanography,* Vol. 34, Pergamon, 45–78.

——, G. Eldin, and K. Wyrtki, 1986: Sea level and dynamic topography in the western Pacific during 1982–83 El Niño. *Trop. Ocean–Atmos. Newsl.,* **36,** 1–3.

Emery, W. J., and L. J. Dewar, 1982: *Mean Temperature–Salinity, Salinity–Depth, and Temperature–Depth Curves in the North Atlantic and North Pacific.* Vol. 3. Pergamon Press, 91 pp.

Godfrey, J. S., and E. J. Lindstrom, 1989: The heat budget of the equatorial western Pacific surface mixed layer. *J. Geophys. Res.,* **94** (C6), 8007–8017.

Gouriou, Y., and J. Toole, 1993: Mean circulation of the upper layers of the western equatorial Pacific Ocean. *J. Geophys. Res.,* **98** (C12), 22 495–22 520.

Huyer, A., P. M. Kosro, R. Lukas, and P. Hacker, 1997: Upper ocean thermohaline fields near 2°S, 156°E during the Tropical Ocean–Global Atmosphere–Coupled Ocean–Atmosphere Response Experiment, November 1992 to February 1993. *J. Geophys. Res.,* **102,** 12 749–12 784.

Ji, M., A. Leetmaa, and J. Derber, 1995: An ocean analysis system for seasonal to interannual climate studies. *Mon. Wea. Rev.,* **123,** 460–481.

——, R. W. Reynolds, and D. Behringer, 1999: Use of TOPEX/Poseidon sea level data for ocean analysis and ENSO prediction: Some early results. *J. Climate,* in press.

Katz, E. J., A. Busalacchi, M. Bushnell, F. Gonzalez, L. Gourdeau, M. McPhaden, and J. Picaut, 1995: A comparison of the ocean surface height by satellite altimeter, mooring, and inverted echo sounder. *J. Geophys. Res.,* **100,** 25 101–25 108.

Kessler, W. S., and B. A. Taft, 1987: Dynamic heights and zonal geostrophic transports in the central tropical Pacific during 1979–84. *J. Phys. Oceanogr.,* **17,** 97–122.

Levitus, S., and T. P. Boyer, 1994: *Temperature.* Vol. 4, *World Ocean Atlas 1994, NOAA Atlas NESDIS 3,* 117 pp.

——, R. Burgett, and T. P. Boyer, 1994: *Salinity.* Vol. 3, *World Ocean Atlas 1994, NOAA Atlas NESDIS 3,* 97 pp.

Lukas, R., 1986: The termination of the equatorial undercurrent in the eastern Pacific. *Progress in Oceanography,* Vol. 23, Pergamon, **16,** 63–90.

——, and E. Lindstrom, 1991: The mixed layer of the western equatorial Pacific Ocean. *J. Geophys. Res.,* **96** (Suppl.), 3343–3357.

McPhaden, M. J., and S. P. Hayes, 1990: Variability in the eastern equatorial Pacific during 1986–1988. *J. Geophys. Res.,* **95,** 13 195–13 208.

Miller, R. N., A. J. Busalacchi, and E. C. Hackert, 1995: Sea surface topography fields of the tropical Pacific from data assimilation. *J. Geophys. Res.,* **100,** 13 389–13 425.

Morris, M., D. H. Roemmich, G. Meyers, and R. Weisberg, 1998: Upper ocean heat and freshwater advection in the western Pacific Ocean. *J. Geophys. Res.,* **103** (C6), 13 023–13 039.

Murtugudde, R., and A. Busalacchi, 1998: Salinity effects in a tropical ocean model. *J. Geophys. Res.,* **103** (C2), 3283–3300.

North, G. R., T. L. Bell, R. F. Cahalan, and F. J. Moeng, 1982: Sampling errors in the estimation of empirical orthogonal functions. *Mon. Wea. Rev.,* **110,** 699–706.

Shinoda, T., and R. Lukas, 1995: Lagrangian mixed layer model of the western equatorial Pacific. *J. Geophys. Res.,* **100,** 2523–2541.

Sprintall, J., and M. Tomczak, 1992: Evidence of the barrier layer in the surface layer of the tropics. *J. Geophys. Res.,* **97,** 7305–7316.

Thépaut, J. N., and P. Courtier, 1991: Four-dimensional variational data assimilation using the adjoint of a multilevel primitive equation model. *Quart. J. Roy. Meteor. Soc.,* **117,** 1225–1254.

Tsuchiya, M., 1968: *Upper Waters of the Intertropical Pacific Ocean.* Vol. 4, Johns Hopkins Oceanographic Studies, 50 pp.

——, R. Lukas, A. Fine, E. Firing, and E. Lindstrom, 1989: Source waters of the Pacific equatorial undercurrent. *Progress in Oceanography,* Vol. 16, Pergamon, 101–147.

Vialard, J., and P. Delecluse, 1998a: An OGCM study for the TOGA decade. Part I: Role of salinity in the physics of the western Pacific fresh pool. *J. Phys. Oceanogr.,* **28,** 1071–1088.

——, and ——, 1998b: An OGCM study for the TOGA decade. Part II: Barrier layer formation and variability. *J. Phys. Oceanogr.,* **28,** 1089–1106.

Webster, P. J., and R. Lukas, 1992: TOGA COARE: The Coupled Ocean–Atmosphere Response Experiment. *Bull. Amer. Meteor. Soc.,* **73,** 1377–1416.

Woodgate, R. A., 1997: Can we assimilate temperature data alone into a full equation of state model? *Ocean Modelling* (unpublished manuscripts), **114,** 4–5.

Wooster, W. S., 1969: Equatorial front between Peru and Galápagos. *Deep-Sea Res.*, **16** (Suppl.), 407–419.

Xie, P., and P. A. Arkin, 1997: Global precipitation: A 17-year monthly analysis based on gauge observations, satellite estimates, and numerical model outputs. *Bull. Amer. Meteor. Soc.*, **78,** 2539–2558.

You, Y., 1998: Rain-formed barrier layer of the western equatorial Pacific warm pool: A case study. *J. Geophys. Res.*, **103** (C3), 5361–5378.